

Article

A New Perspective on HCl Scavenging at High Temperatures for Reducing the Smoke Acidity of PVC Cables in Fires. II: Some Examples of Acid Scavengers at High Temperatures in the Condensed Phase

Gianluca Sarti ^{2,*}¹ Reagens S.p.A.; gianluca.sartieagens-group.com

* Correspondence: gianluca.sartieagens-group.com

Abstract: in the European Union, according to Regulation (EU) n. 305/11 (Construction Product Regulation, or CPR), cables permanently installed in buildings need additional classification for acidity, performing EN 60754-2. The research on PVC compounds with low smoke acidity helps to produce cables in the best additional classes for acidity, giving the PVC cables the possibility to be used in medium and high fire risk locations. In this paper, some acid scavengers at high temperatures are tested to verify their possible scavenging mechanism and their efficiency in performing EN 60754-2 at different temperatures.

Keywords: acid scavengers; PVC; cables; smoke acidity

1. Introduction

In 2006 separate classes of reaction-to-fire performance were established for electric cables, including the additional classification for acidity, according to the Commission Decision of 27 October 2006, amending the Decision 2000/147/EC and implementing Council Directive 89/106/EEC, called Construction Product Directive or just CPD. At that time, the test method used to assess acidity was EN 50267-2-3. Since Construction Product Regulation (Regulation (EU) n. 305/2011, or CPR) entered into force in 2017, EN 50267-2-3 has become the test method for assessing smoke acidity, followed by EN 60754-2. EN 60754-2, EN 60754-1 (and their siblings EN 50267-2-2 and EN 50267-2-1) are used in EN 50525 series (see EN 50525-1, annex B, table B2) to assess if a compound could be considered "halogen-free," therefore both are standard test methods used by halogen-free producers. The paradox is that while EN 60754-1 is a well-known and corroborated test method for PVC compound producers, EN 60754-2 is entirely unknown to them. The result is a historical lack of data on the pH and conductivities of PVC compounds for cables and difficulties in understanding how the classes a2 and a1 can be reached. The use of acid scavengers in PVC compounds has a long historical tradition. PVC compounds with low smoke acidity are mandatory in some locations where a substantial reduction of smoke acidity is required (i.e., ENI 0181.00). Some acid scavengers at high temperatures are special calcium carbonates with fine particle sizes. Especially precipitated calcium carbonate (PCC) was and still is the more suitable calcium carbonate for

getting down the smoke acidity of PVC compounds. Still, other extremely fine ground calcium carbonates (GCCs) can be used. The paper shows the behavior of 5 acid scavengers, alone and in combinations, performing EN 60754-2 in isothermal conditions for 30 minutes at 400°C, 500°C, 600°C, 800°C, and 955°C. It focuses on the performances at different temperatures and shows how, if an acid scavenger is present, the higher the temperature, the lower the efficiency. This part shows new data clarifying aspects presented in a series of conferences between 2017 and 2022, particularly AMI cables 2019, AMI cables 2020, and AMI formulation 2021. Those conferences, the regulatory context, and the research on low smoke acidity PVC compounds are well described in this letter [1].

2. Materials and Methods

2.1 Materials

Table 1 shows the first series of formulations. The amount of ingredients is expressed per hundred resin (phr). They have been tested according to internal method 2, indicated in Table 6.

Table 1. First series of formulations: COS stands for Calcium Organic Stabilizer, AS-1 and AS-6B are acid scavengers at high temperatures developed by Reagens S.p.A.

Raw Materials	Trade name	F50.0 [phr]	F50.1 [phr]	F50.2 [phr]	F50.3 [phr]	F50.4 [phr]	F50.5 [phr]
PVC	Inovyn 271 PC	100	100	100	100	100	100
DINP	Diplast N	50	50	50	50	50	50
ESBO	Reaflex EP6	2	2	2	2	2	2
Antioxidant	Arenox A10	0.1	0.1	0.1	0.1	0.1	0.1
COS	RPK B-CV 3037	3	3	3	3	3	3
CaCO ₃	Riochim	90	0	0	0	0	0
Al(OH) ₃	Apyral 40 CD	0	90	0	0	0	0
Mg(OH) ₂	Ecopyren 3.5	0	0	90	0	0	0
PCC	Winnofl S	0	0	0	90	0	0
HTAS 1	AS-1	0	0	0	0	90	0
HTAS 2	AS-6B	0	0	0	0	0	90

Table 2. Second series of formulations. pH and conductivity are measured according to EN 60754-2 at 950°C.

Raw Materials	Trade name	F50.6 [phr]	F50.7 [phr]	F50.8 [phr]	F50.9 [phr]	F50.10 [phr]
PVC	Inovyn 271 PC	100	100	100	100	100
DINP	Diplast N	50	50	50	50	50
ESBO	Reaflex EP6	2	2	2	2	2
IX1010	Arenox A10	0.1	0.1	0.1	0.1	0.1
COS	RPK B-CV 3037	3	3	3	3	3
CaCO ₃	Riochim	0	0	0	0	0
Al(OH) ₃	Apyral 40 CD	0	0	0	0	0
Mg(OH) ₂	Ecopyren 3.5	0	130	40	80	104
PCC	Winnofl S	130	0	90	180	234

The formulations in Table 2 are designed to test the effect on the efficiency of PCC and $Mg(OH)_2$ at high loading levels. Here we focused on the synergism and the increase of smoke acidity due to dispersion phenomena.

Table 3 shows the third series of formulations used to focus on the $Mg(OH)_2$ / PCC synergism.

Table 3. Synergism of PCC/ $Mg(OH)_2$ couple. The measures are performed according to EN 60754-2 at 950°C.

Raw Materials	Trade name	50.6	50.7	50.18	50.8	50.19	50.20	50.21	50.22	50.23
		[phr]	[phr]	[phr]	[phr]	[phr]	[phr]	[phr]	[phr]	[phr]
PVC	Inovyn 271 PC	100	100	100	100	100	100	100	100	100
DINP	Diplast N	50	50	50	50	50	50	50	50	50
ESBO	Reaflex EP6	2	2	2	2	2	2	2	2	2
IX1010	Arenox A10	0.1	0.1	0.1	0.1	0.1	0.1	0.1	0.1	0.1
COS	RPK B-CV 3037	3	3	3	3	3	3	3	3	3
$Mg(OH)_2$	Ecopyren 3.5	0	130	30	40	90	100	0	0	0
PCC	Winnofl S	130	0	100	90	40	30	100	90	40

The following materials have been used to perform EN 60754-2: Double Deionized Water (DDW) is internally produced by an ion exchange deionizer. The pH of DDW must be between 5,50 and 7,50, and the conductivity less than $0.5 \mu S/mm$. Buffer and conductivity standard solutions come from VWR International (pH: 2.00, 4.01, 7.00, and 10.00, conductivity: 1.5, 8.4, 14.7, 141.3 $\mu S/mm$).

2.2 Test Apparatus

Table 4 gives the list of utilized test apparatuses.

Table 4. Main test apparatuses utilized.

Test apparatus	Producer	model	Additional Infos
Plasticorder	Brabender		50 CC, chamber
Thermostat	Liebisch Labortechnik	LT-PVC-210-36-5	according to EN60811-405
Halogen Acid Gas test apparatus	SA Associates		
Multimeter	Mettler Toledo	S213 standard kit	
Conductivity electrode	Mettler Toledo	S213 standard kit	
pH electrode	Mettler Toledo	S213 standard kit	
FTIR-ATR	Thermo	IS20	
WD-XRF	Thermo		
Dynamometer	Hounsfield	H10KS	Specimen type 1A, 500 mm/min

2.3 Sample preparation

PVC compound samples are prepared by weighing the stabilizers' ingredients in the 0.001 g balance. PVC, plasticizers, fillers, flame retardants, and acid scavengers are weighed in the 0.1 g balance. PVC and all the ingredients are mixed in a 20 L turbo-mixer up to 105°C, producing 3 Kg dry-blend batches. The dry blend is processed in the plasticorder for 10 minutes at 160°C, 30 rpm, getting 60 g kneaders. The kneaders are pressed at 160°C for 3 minutes in 0.5 mm, 1 mm, and 6 mm sheets from which test specimens are obtained for the tests indicated in Tables 5 and 6.

2.4. Internal tests and international technical standards used

Tables 5 and 6 recall the used technical standards.

Table 5. Tests for the type of compound.

Technical standard	Measurement	Temperature	Note
ISO 527	Elongation at break	23°C	Test specimens conditioned per 24 h at 23°C
ISO 527	Tensile strength	23°C	Test specimens conditioned per 24 h at 23°C
ISO 1183	Specific Gravity	23°C	After 24 h of storage at 23°C
ISO 868	Hardness	23°C	SHA at 15", after 24 h of storage at 23°C
IEC 60811 – 405	Thermal Stability	200°C	Test specimens conditioned per 24 h at 23°C

Table 6. Tests for acidity assessment.

Technical standard	Measurement	Temperature [°C]	Note
EN 60754 – 2	Smoke acidity	950	DDW, pH, and conductivity, general method
Internal Method 2	Smoke acidity	400, 500, 600, 800, 950	DDW, pH and conductivity

General method of EN 60754-2 is performed as follows: a calibrated reference thermocouple is used to control the temperature. The probe is introduced in the central part of the quartz glass tube, where an empty combustion boat is carried from the sample carrier. The temperature measured by the reference thermocouple is adjusted to 950 +/- 5 °C, maintaining it for at least one hour. The furnace tube is ready for the first run when the temperature is stable. Then, a sample of 1.000 +/- 0.001 g is weighed in a combustion boat. The porcelain combustion boat has dimensions according to the standard. It is introduced directly into the quartz glass tube, moving the magnet along the sample carrier, while the countdown is activated when the combustion boat reaches the central part of the quartz glass tube. The smokes are purged in the bubbling devices containing DDW for 30 min by a normalized air flux (set according to the standard EN 60754-2 considering the geometry of the quartz glass tube). After 30 minutes, the connectors are disconnected, and the magnet extracts the combustion boat from the quartz glass tube. The water collected by the bubbling devices is brought at 1 L, and pH and conductivity are measured. The precautions indicated in Part I of this manuscript have been adopted to minimize the errors, which lead to poor repeatability and reproducibility.

Internal method 2 is performed as EN 60754-2 but applies different isothermal profiles. That procedure permits the evaluation of the efficiency of an acid scavenger at different temperatures. The efficiency is calculated as indicated in Part I of this paper. pH and conductivity measures are taken at 25°C +/- 1 with the following procedure: the multi-meter is calibrated with standard solutions before each measurement. The pH is calibrated at two points (4.01 and 7.00). Conductivity is calibrated at 1 point at 141.3 µS/mm. The solutions closer to the measured value are chosen as correction standards, and the measurements are corrected accordingly through a correction factor. pH and conductivity electrodes have a reference thermocouple that adjusts the fluctuation of temperature.

The smoke acidity measurements usually have a low grade of repeatability, especially if the temperature is high. This weakness is intrinsic to dynamics affecting the burning of the sample in a furnace tube. Samples do not burn the same way, and passivation can lead to some fluctuations in the results. Furthermore, as indicated in Part 1 of this manuscript, most procedures are done manually, which is the most significant source of errors. Therefore, a series of five measurements for each sample is performed, and this statistical method is used to calculate the mean value and outliers: from the five test determinations, the mean value μ , standard deviation s , and coefficient of variation CV are calculated for pH and conductivity using the following formulations:

$$\mu = \sum_{i=1}^N \frac{x_i}{N} \quad (1)$$

$$s = \sqrt{\frac{\sum_{i=1}^N (\mu - x_i)^2}{N-1}} \quad (2)$$

$$CV = \frac{\mu}{s} \quad (3)$$

If the CV is higher than 5 %, a further five measurements are performed, and the mean value, standard deviation, and coefficient of variation are recalculated.

3. Results

3.1 First series of formulations

Table 7 shows the main properties of the first series of formulations. The main properties indicate if the compound is suitable for manufacturing insulation, jacket, or bedding.

Table 7. Focus on the main properties of the compounds.

Formulation →	F50.0	F50.1	F50.2	F50.3	F50.4	F50.5
Specific Gravity [g/cm ³]	1.542	1.505	1.503	1.542	1.445	1.446
Hardness [SHA 15"]	88	89	89	88	90	90
Tensile strength [N/mm ²]	13.0	11.8	11.7	13.4	13.0	13.1
Elongation at break [%]	246	236	233	240	221	225
Thermal Stability [min]	104	79	73	76	291	299

Internal method 2 has been performed at different temperatures, 400°C, 500°C, 600°C, 800°C, and 950°C and Table 8 shows the results of pH and conductivity for each formulation. Table 9 reports the elements found in ashes determined by XRF spectrometry. Figures 1–6 show the FTIR spectra of the ashes of F50.0 – F50.5 at different temperatures. Figure 7-11 display the FTIR spectra of some standards compared to some ashes of F50.0 – F50.5. Table 10 gives the principal FTIR bands of the substances found in the ashes.

The ashes are analyzed through the following procedure. After the combustion boat is extracted from the furnace tube, it is left to cool down and put in a PE zip lock bag. Before the measurement, the combustion boat is dried for 2 hours in the oven at 105°C. Metal oxides or chlorides are in the ash residue and are highly hygroscopic. XRF is conducted using borate-fused beads.

Table 8. pH and conductivities at 400 °C.

Method 2 @ 400°C	F50.0	F50.1	F50.2	F50.3	F50.4	F50.5
pH	2.48	2.37	2.81	3.71	4.03	3.88
Conductivity [$\mu\text{S}/\text{mm}$]	142.9	179.4	88.7	8.1	4.0	5.3
Method 2 @ 500°C	F50.0	F50.1	F50.2	F50.3	F50.4	F50.5
pH	2.48	2.41	2.41	3.73	3.70	3.69
Conductivity [$\mu\text{S}/\text{mm}$]	139.1	177.2	177.3	7.7	8.2	8.6
Method 2 @ 600°C	F50.0	F50.1	F50.2	F50.3	F50.4	F50.5
pH	2.51	2.30	2.31	3.69	3.70	3.65
Conductivity [$\mu\text{S}/\text{mm}$]	132.6	201.7	195.7	9.2	7.8	9.5
Method 2 @ 800°C	F50.0	F50.1	F50.2	F50.3	F50.4	F50.5
pH	2.63	2.30	2.29	3.26	3.52	3.20
Conductivity [$\mu\text{S}/\text{mm}$]	100.4	206.4	208.9	23.7	13.5	25.7
Method 2 @ 950°C	F50.0	F50.1	F50.2	F50.3	F50.4	F50.5
pH	2.62	2.26	2.25	2.75	2.78	2.77
Conductivity [$\mu\text{S}/\text{mm}$]	97.3	221.5	224.3	74.0	70.1	70.1

Table 9. Main elements in ashes detected by XRF.

Formulation →	F50.0	F50.1	F50.2	F50.3	F50.4	F50.5
400°C	Ca, Cl	Mg, Cl	Al, Cl	Ca, Cl	n.a.	n.a.
500°C	Ca, Cl	Mg, Cl	Al, Cl	Ca, Cl	n.a.	n.a.
600°C	Ca, Cl	Mg, Cl	Al, Cl	Ca, Cl	n.a.	n.a.
800°C	Ca, Cl	Mg, Cl	Al, Cl	Ca, Cl	n.a.	n.a.
955°C	n.a.	n.a.	n.a.	n.a.	n.a.	n.a.

n.a. = not available

Table 10. Main FTIR bands detected in the ashes.

Formulation →	1 [cm^{-1}]	2 [cm^{-1}]	3 [cm^{-1}]	4 [cm^{-1}]	5 [cm^{-1}]	6 [cm^{-1}]
CaCO ₃	2509.64	1794.92	1417.26	873.10	846.70	710.66
MgCl ₂	1616.40	1606.07				
CaCl ₂	1628.43	1614.21				
MgO	Broadband centered at 548 cm^{-1}					
Al ₂ O ₃	Broadband between 400 and 900 cm^{-1}					

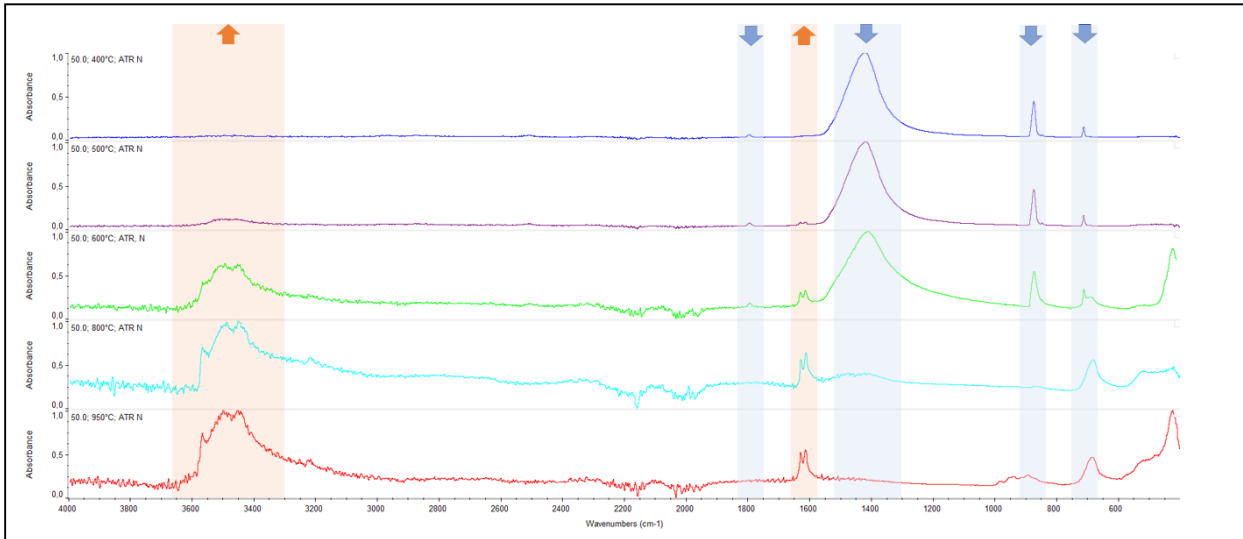


Figure 1. FTIR spectra of ashes of 50.0 at 950°C (red), at 800°C (light-blue), at 600°C (green), at 500°C (purple), at 400°C (blue).

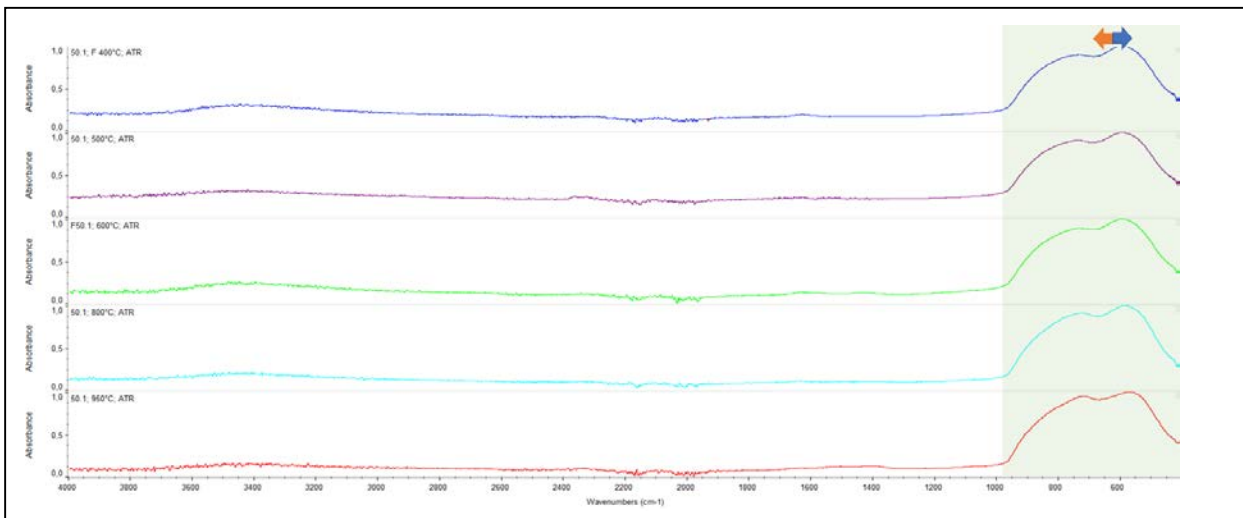


Figure 2. FTIR spectra of ashes of 50.1 at 950°C (red), at 800°C (light-blue), at 600°C (green), at 500°C (purple), at 400°C (blue).

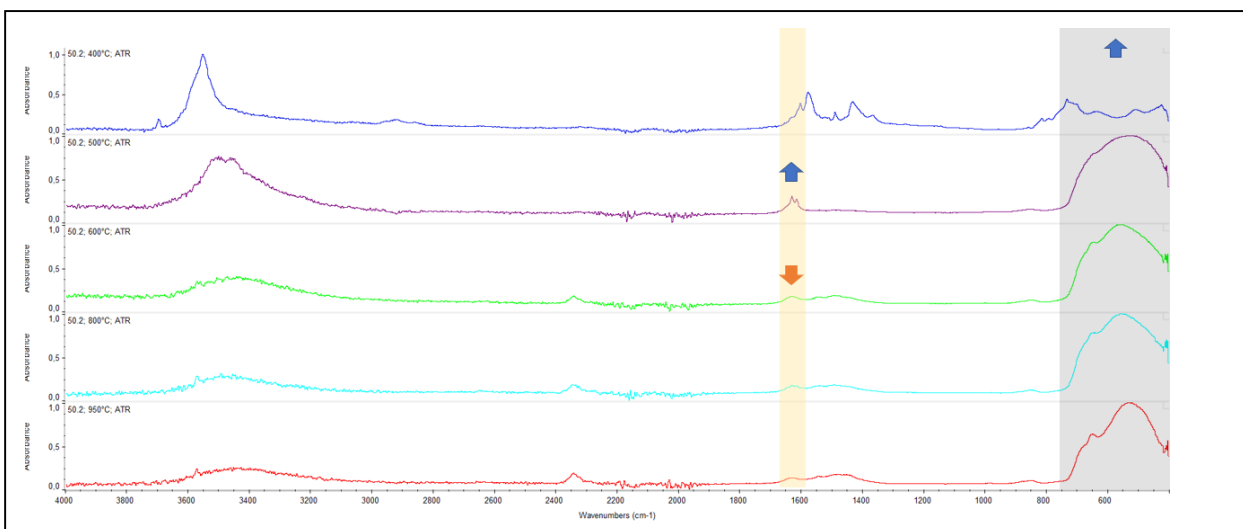


Figure 3. FTIR spectra of ashes of 50.2 at 950°C (red), at 800°C (light-blue), at 600°C (green), at 500°C (purple), at 400°C (blue).

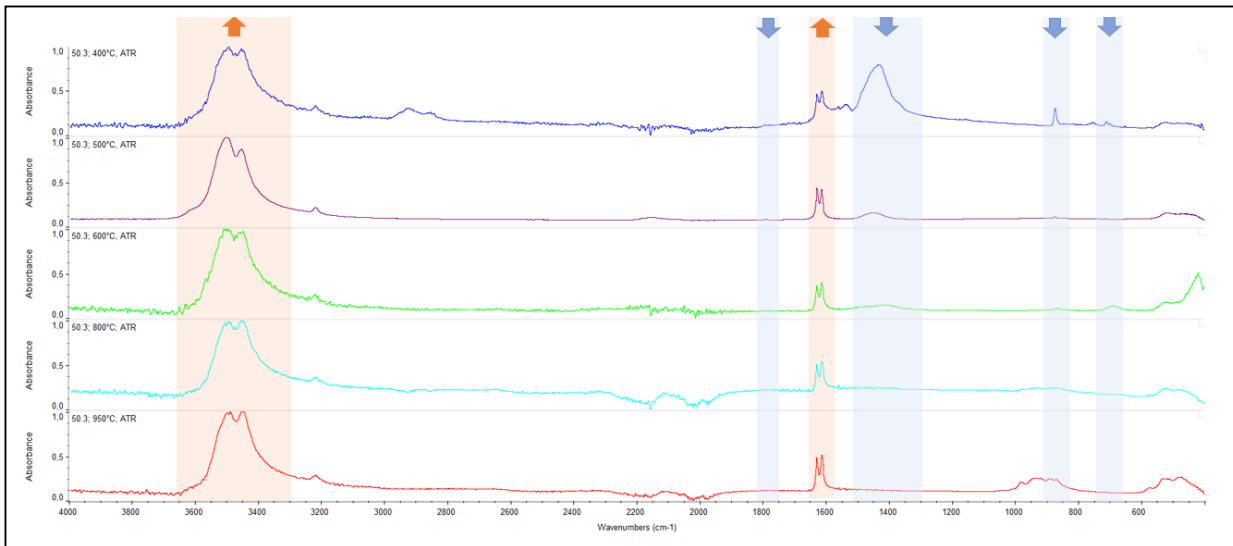


Figure 4. FTIR spectra of ashes of 50.3 at 950°C (red), at 800°C (light-blue), at 600°C (green), at 500°C (purple), at 400°C (blue).

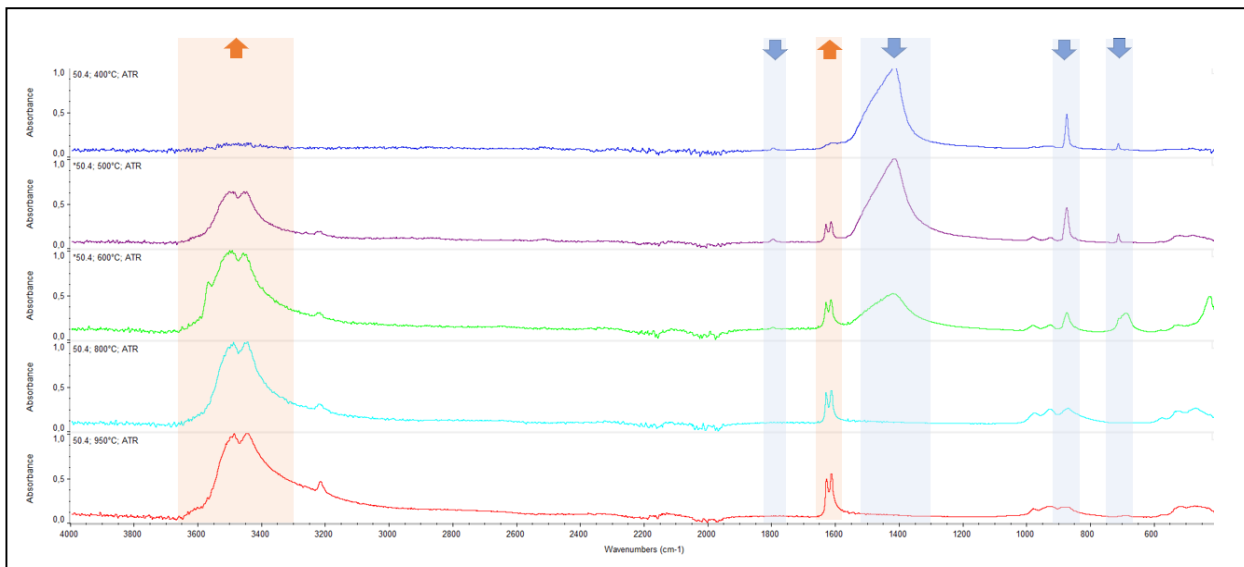


Figure 5. FTIR spectra of ashes of 50.4 at 950°C (red), at 800°C (light-blue), at 600°C (green), at 500°C (purple), at 400°C (blue).

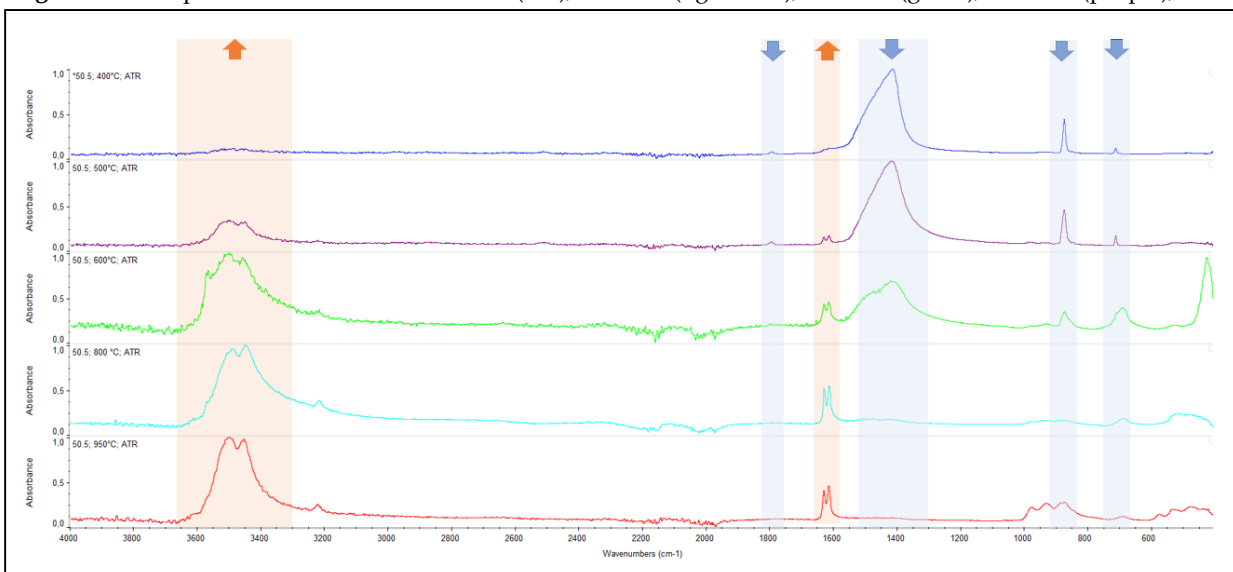


Figure 6. FTIR spectra of ashes of 50.5 at 950°C (red), at 800°C (light-blue), at 600°C (green), at 500°C (purple), at 400°C (blue).

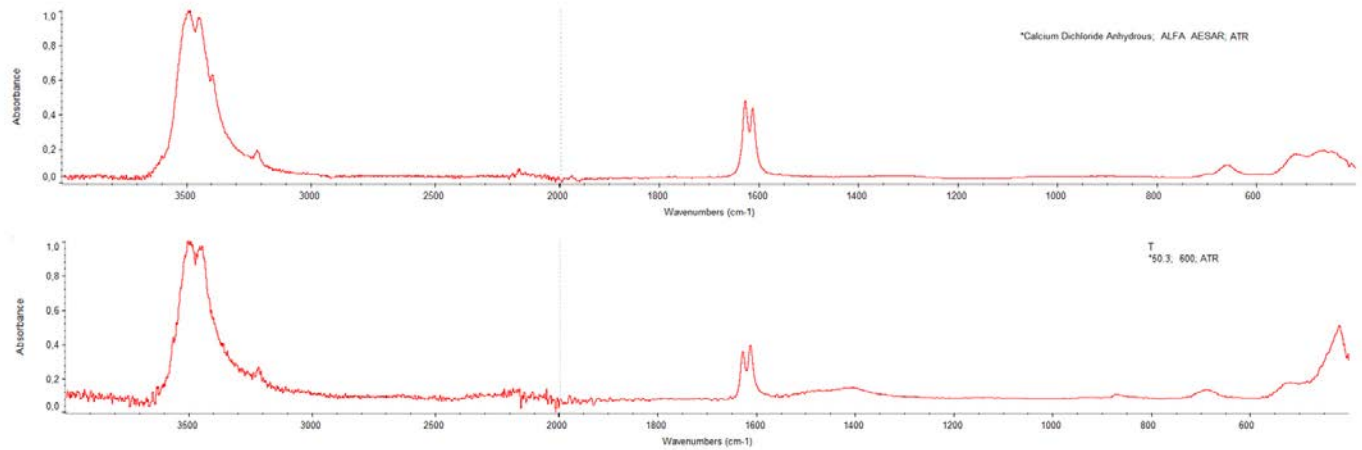


Figure 7. CaCl₂ FTIR spectrum: standard vs F.50.3 ashes at 600°C.

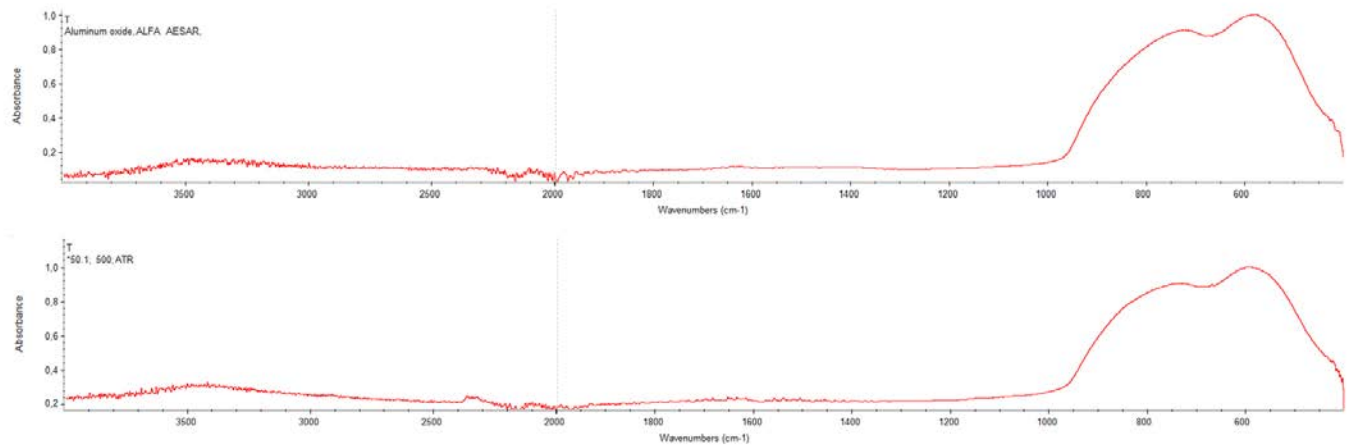


Figure 8. Al₂O₃ FTIR spectrum: standard vs. F50.1 ashes at 500°C.

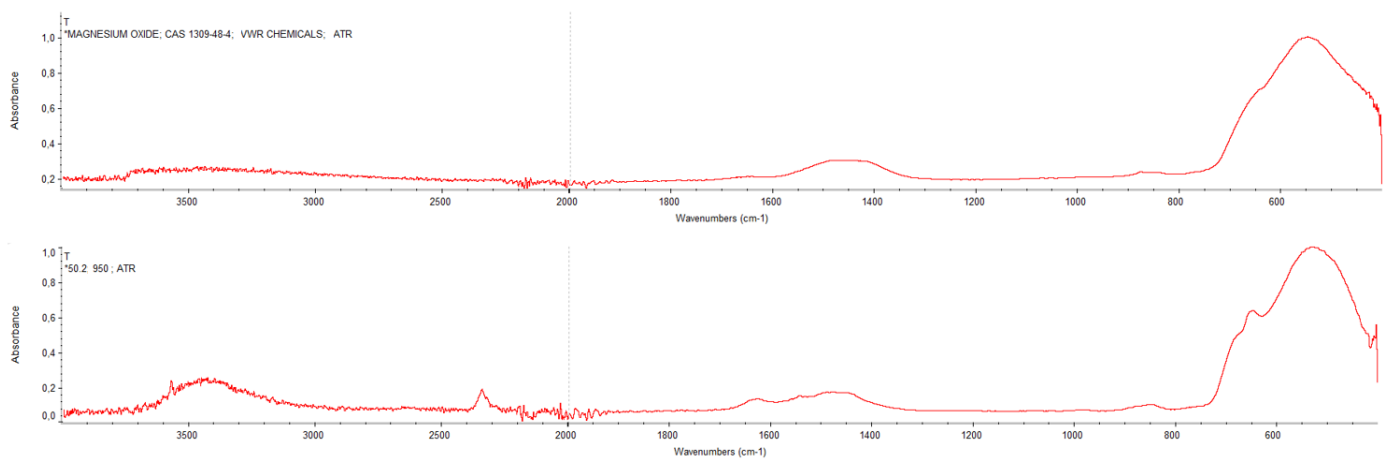


Figure 9. MgO FTIR spectrum: standard vs F50.2 ashes at 950 °C.

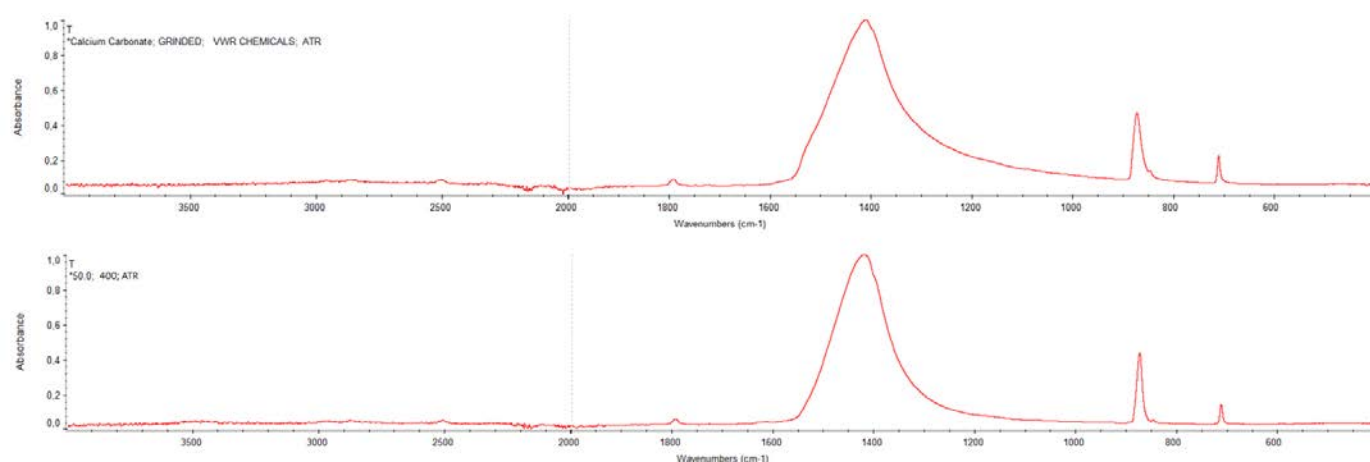


Figure 10: CaCO₃ FTIR spectrum: standard vs F50.0 ashes at 400 °C.

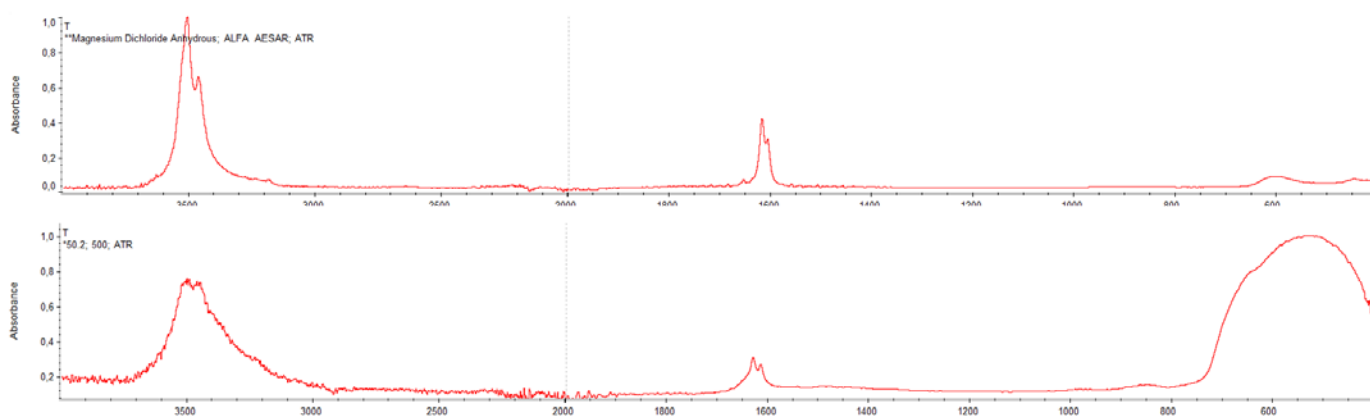


Figure 11: MgCl₂ FTIR spectrum: standard vs F50.2 ashes @ 500 °C

3.2 Second series of formulations

Table 11 shows the pH and conductivity of the second series of formulations used to evidence the Mg(OH)₂/PCC synergism.

Table 11. Synergism of PCC/Mg(OH)₂ couple. The measures are performed according to EN 60754-2 at 950°C.

Formulation	F50.6	F50.7	F50.18	F50.9	F50.19	F50.20	F50.21	F50.22	F50.23
pH	2.93	2.28	3.19	3.75	2.65	2.51	2.90	2.89	2.33
Conductivity [μS/mm]	49.4	183.8	28.8	8.36	106.2	133.5	56.9	51.6	193.0

3.3 Third series of formulations

Table 12 shows the main properties of the formulations 50.6 – 50.10 and pH and conductivities, focusing on the couple PCC / Mg(OH)₂ and the effect of its high loading level on acidity (collapse of the smoke acidity performance due to the reduced dispersion of both additives). The smoke acidity has been measured using EN 60754-2 at 950°C.

Table 12. Third series of formulations. pH, conductivity, and the main properties of the compound.

Formulation	F50.6	F50.7	F50.8	F50.9	F50.10
pH	2.93	2.34	3.32	3.75	3.75
Conductivity [$\mu\text{S}/\text{mm}$]	49.4	183.8	20.7	8.36	8.35
Specific Gravity [g/cm^3]	1.644	1.590	1.627	1.853	1.946
Hardness [SHA 15"]	91	92	91	97	98
Tensile strength [N/mm^2]	8.2	5.8	7.5	2.3	1.2
Elongation at break [%]	210	195	205	177	172
Thermal Stability [min]	76	71	61	57	38

3.4 The efficiency of scavenging

Tables 13, 14, and 15 display the efficiency values of F50.0 – F50.5, performing internal method 2 at the indicated temperatures.

Table 13. The efficiency [%] of formulations F50.0 - F50.5: EN60754-2 at different temperatures.

Temperature [$^{\circ}\text{C}$]	F50.0	F50.1	F50.2	F50.3	F50.4	F50.5
400	8.0	5.1	16.9	40.0	50.8	45.1
500	8.1	6.3	6.3	40.6	41.8	40.2
600	8.6	3.1	3.4	39.7	40.9	38.9
800	12.0	3.3	3.1	28.2	36.9	27.1
950	12.2	2.4	2.3	14.7	18.7	16.0

Table 14. The efficiency [%] of formulations F50.6 - F50.10: EN60754-2 at 950 $^{\circ}\text{C}$.

	F50.6	F50.7	F50.8	F50.9	F50.10
950 $^{\circ}\text{C}$	18.4	2.4	28.8	37.5	34.9

Table 15. The efficiency [%] of formulations F50.18 - F50.23: EN60754-2 at 950 $^{\circ}\text{C}$.

	F50.18	F50.19	F50.20	F50.21	F50.22	F50.23
950 $^{\circ}\text{C}$	25.2	10.8	7.0	18.5	18.6	6.3

4. Discussion

4.1 Effect of chemical properties of a substance on efficiency

The chemical properties of acid scavengers greatly influence efficiency. For example, AS-6B (a mix of basic substances) shows higher efficiency than ground calcium carbonate (GCC) or $\text{Al}(\text{OH})_3$ (Tables 8 and 13). That confirms what was outlined by O'Mara in [2] and Brown and Martin in [3]. Thus, substances with high reactivity with HCl are always a good starting point for their evaluation as acid scavengers at high temperatures. Figure 12 shows the efficiency of AS-6B, GCC, and $\text{Al}(\text{OH})_3$ at different temperatures, performing internal method 2.

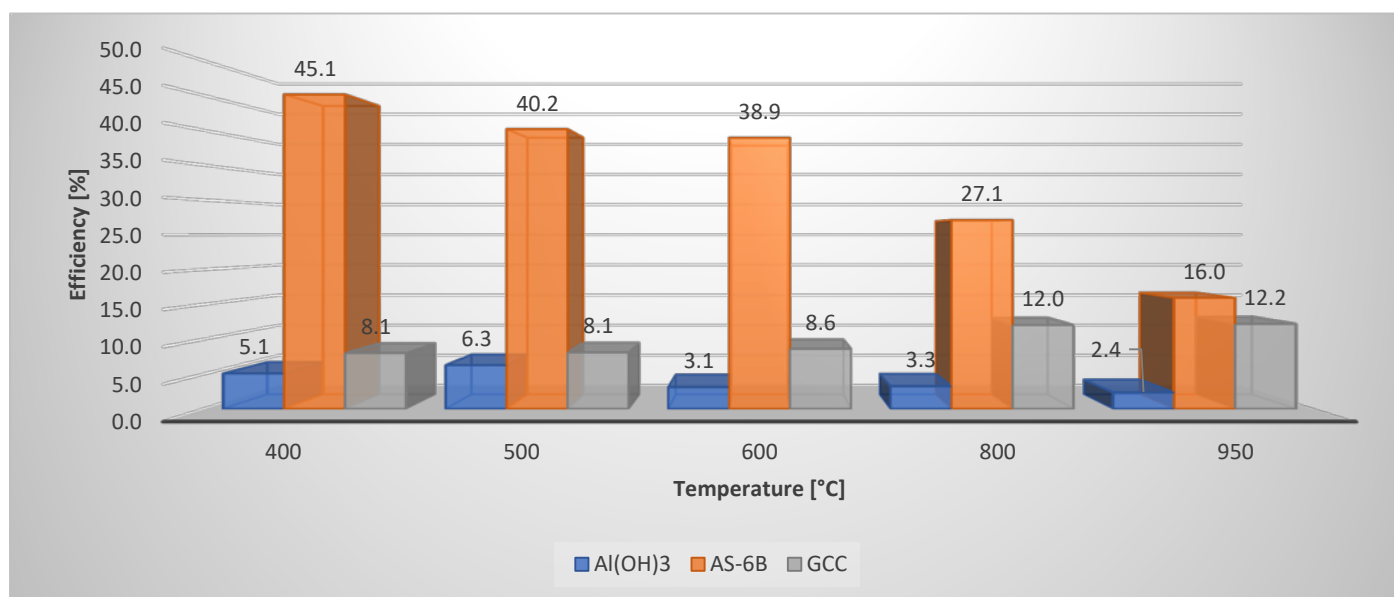


Figure 12. Efficiency (T) of F50.5 (Orange), F50.3 (Yellow), and F50.2 (Blue).

PCC and $\text{Al}(\text{OH})_3$, respectively.

4.2 Effect of particle size on efficiency

GCC has less efficiency than PCC (Table 8 and Table 13), which is valid for all temperatures. F50.0 contains a GCC with a mean particle size of 10 microns, while F50.3 has Winnofil S, a PCC having a particle size in the scale of nanometers and a BET between $15 \text{ m}^2/\text{g}$ and $24 \text{ m}^2/\text{g}$ [4]. O'Mara made the same assumption without any measurement in [2], claiming that the Molar Absorption Efficiency (MAE) depends on several variables, such as acid scavengers' dispersion efficiency and particle size. Matthews and Plemper in [5, 6] have shown how the reactivity of CaCO_3 is linked to particle size, and it can cause a substantial effect on flame retardancy. We will discuss this aspect in detail in Part IV of this paper.

In conclusion, substances with finer particle sizes show more reactivity with HCl than small ones because of a higher BET, which means more probability of intercepting gaseous HCl molecules. For this reason, PCC is more performant in scavenging than GCC.

One of the points to be highlighted is that the advantage of PCC is reduced as temperature increases, moreover at $950 \text{ }^\circ\text{C}$, when all acid scavengers at high temperatures cannot compete with the fast evolution of HCl (Table 13, Figure 12 and 13).

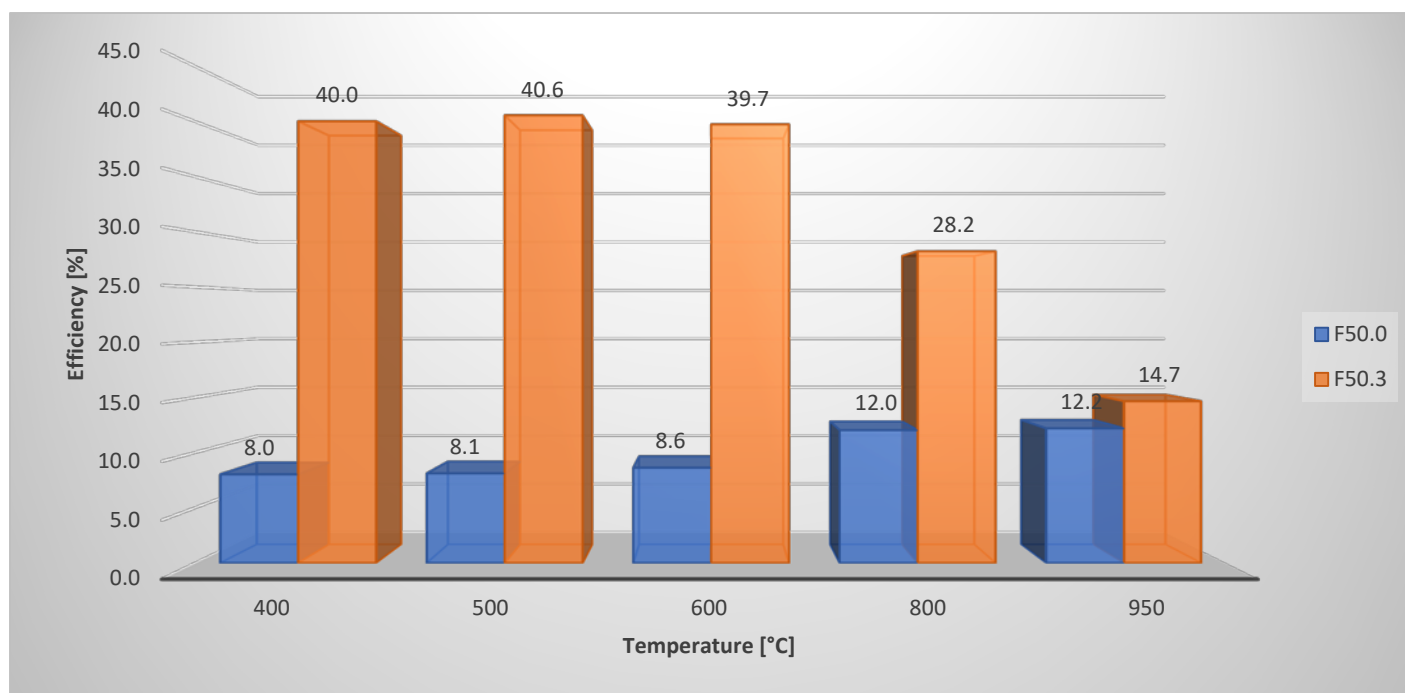


Figure 13. The efficiency (T) of F50.0, containing 90 phr of GCC, and F50.3, containing 90 phr of PCC.

4.3 Effect of dispersion on efficiency

The formulation F50.8 contains PCC and $\text{Mg}(\text{OH})_2$, 90 phr, and 40 phr, respectively, with a ratio of PCC / $\text{Mg}(\text{OH})_2$ of 2.25. That is the best ratio found for the best efficiency. The efficiency of this acid scavenger couple is 28.8 % (Table 14, Figure 14), with a pH of 3.32 (Table 12). By doubling the quantity of the couple with the same ratio, 37.5 % of efficiency with a pH of 3.75 are reached. With a further improvement of the dosage, no further advantages are obtained (Figure 14). This behavior indicates poor dispersion as the dosage increases, impacting the scavenging performances. An inadequate distribution weakens the intimate contact between PVC chains and acid scavengers. If this contact misses in some zones, HCl is released, lowering the efficiency of acid scavengers. Sometimes, it can be compensated by increasing the share during the process and using some tricks during the blending. Nevertheless, nanoscale fillers and substances prone to uptake water, such as $\text{Mg}(\text{OH})_2$, are always inclined to give bad dispersion if we enhance their dosage. O' Mara in [2] claimed the impacts of the dispersion of acid scavengers on their efficiency.

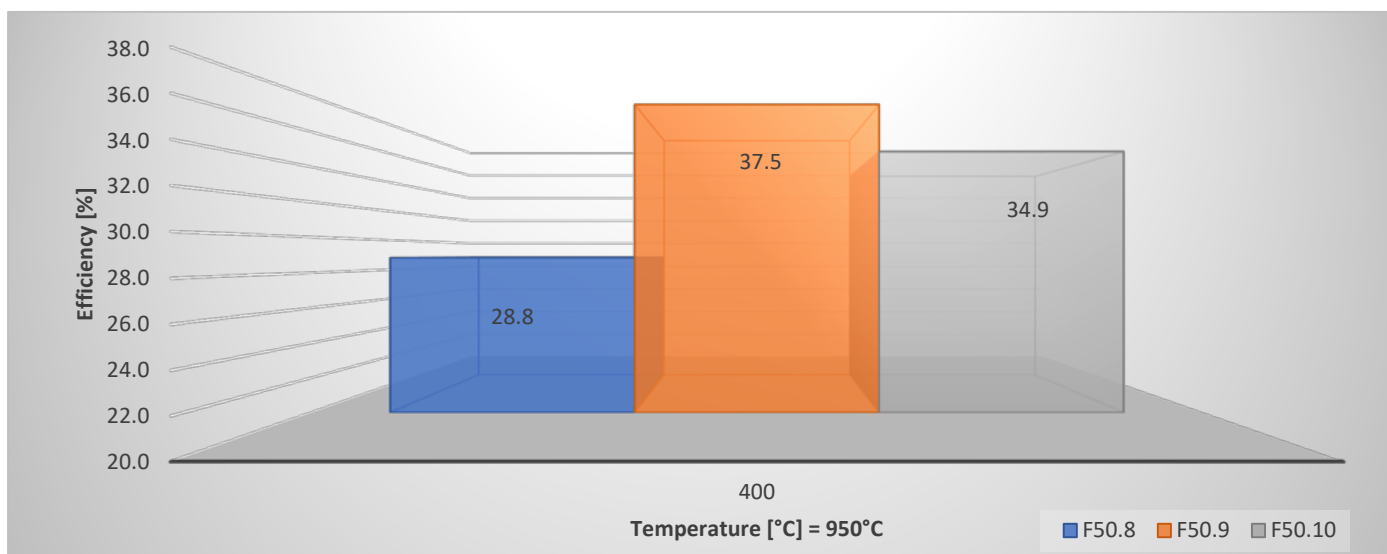


Figure 14. Efficiency (T) of formulations containing PCC/Mg(OH)₂ at different dosages.

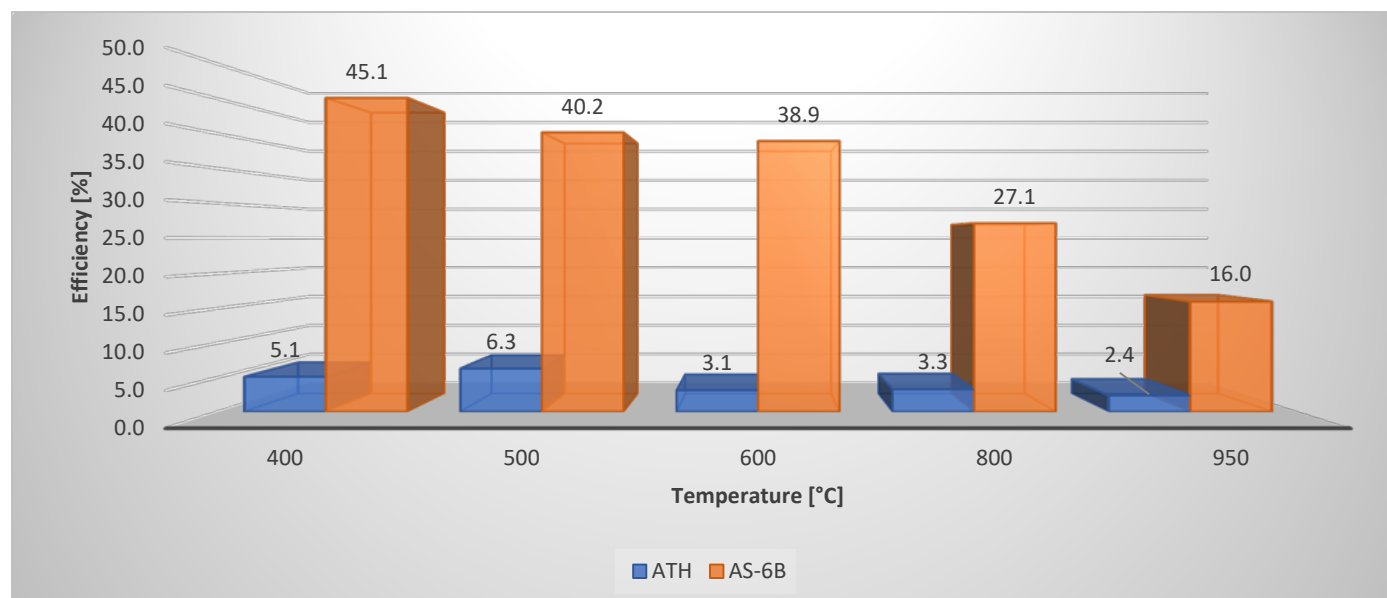


Figure 15. Efficiency (T) of formulation F50.1 (blue) and F50.5 (orange) as a function of temperature.

4.4 Effect of temperature on efficiency

AS-6B gives stable reaction products with HCl, so the efficiency is only due to the kinetic of the reactions involved in trapping HCl. Its acid scavenger efficiency falls dramatically as temperature increases (Figure 15). The efficiency of other good acid scavengers, such as PCC, shows a similar trend (Figure 13). The explanation lies in the competition between two reactions. HCl evolves from the burning matrix, and acid scavengers try to fix it in ashes. The higher the temperature, the quicker the evolution of HCl. Over certain temperatures, solid acid scavenger becomes too slow to trap HCl efficiently, and the system goes into crisis. Chandler and alt. in [7] and Bassi in [8] highlighted this phenomenon. Finally, a non-performant acid scavenger such as Al(OH)₃ has terrible behavior at all tested temperatures.

4.5 Effect of decomposition of reaction products on efficiency

Kipouros and Sadoway claimed the MgCl_2 decomposition last step at 550°C [9]. Galwey and Lavery between 350°C and 550°C [10]. The efficiencies reported in Figure 16 and FTIR spectra in Figure 3, confirm that over 400°C , MgCl_2 decomposes. The ashes at 400°C are black, and the FTIR spectrum at 400°C shows the presence of an unknown substance, probably a mix of a variety of crosslinked organic compounds forming a black and solid char. Here the second stage of pyrolysis and combustion zone starts, and the formation and rearrangement of the crosslinked matrix are expected. However, the FTIR spectrum shows the presence of weak MgCl_2 bands at 1616.4 cm^{-1} and 1606.1 cm^{-1} , confirming that MgCl_2 is diluted in the black char (Figure 3 and Table 10). The signal of the organic crosslinked char entirely disappears at 500°C , and therefore the MgCl_2 bands become evident. Nevertheless, at 500°C , the principal band at 546.2 cm^{-1} confirms the presence of MgO (Figures 3, 9, 11, and Tables 9 and 10). MgCl_2 bands vanish completely at 600°C , where MgO is the only source of Mg (Figures 3 and 11 and Tables 9 and 10). The decomposition of MgCl_2 is why the efficiency of $\text{Mg}(\text{OH})_2$ decreases after 400°C . Therefore, by performing internal method 2, $\text{Mg}(\text{OH})_2$ shows the maximum efficiency at 400°C (16.9 %), and its efficiency drops to 2.3 % at 950°C .

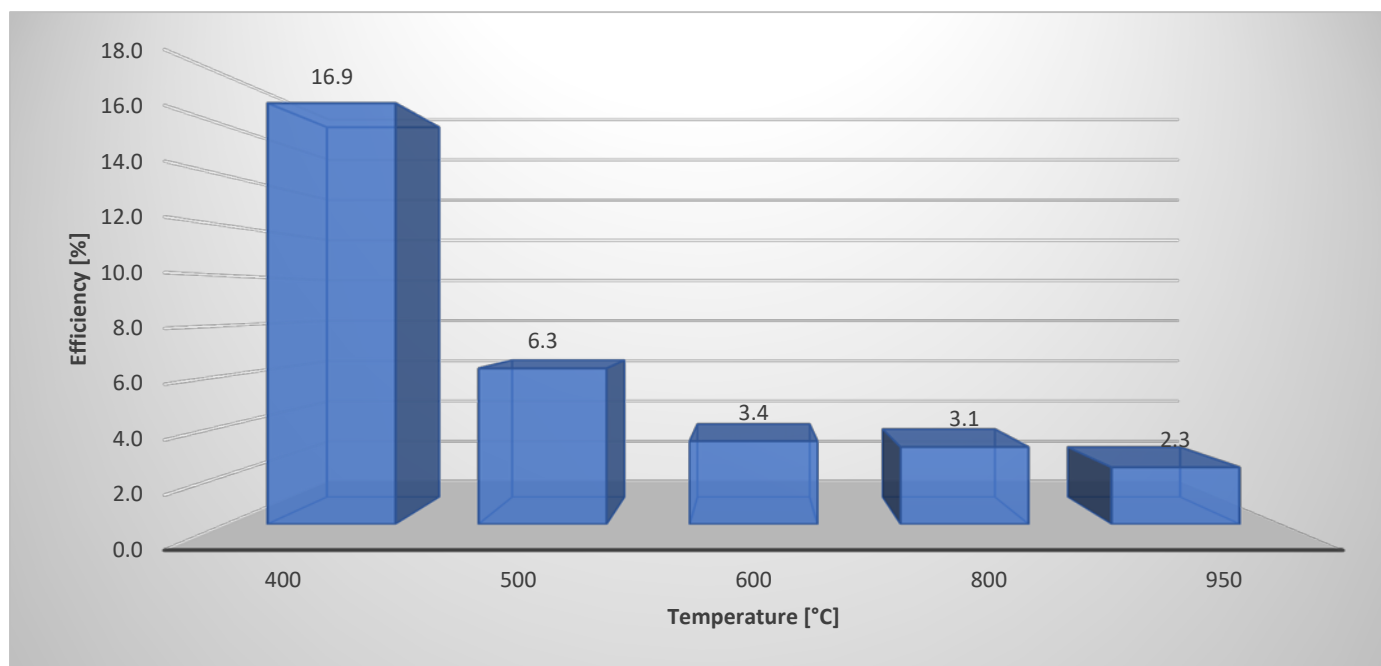


Figure 16. Efficiency (T) of the formulation F50.2 containing $\text{Mg}(\text{OH})_2$.

4.6 Focus on the single acid scavengers

4.6.1 Single step reaction: GCC

GCC reacts with HCl in a single-step reaction, yielding CaCl_2 , CO_2 , and water. Its reaction product, CaCl_2 , is stable up to 950°C . The efficiency of GCC in F50.0 remains low, slightly increasing from 400°C to 950°C (Table 13), probably due to the formation of small quantities of CaO , which is more likely to happen at 800°C and 950°C and acts as a potent acid scavenger. This phenomenon gives a slight advantage to all kinds of CaCO_3 in the scavenging at temperatures over 800°C . In PCC, this advantage is not visible (F50.3) because "covered" by PCC's high scavenging performances. FTIR (Figure 1, 7, 10, and Table 10) and XFR (Table 9) point to the involved reactions. At 400°C , 500°C , and 600°C , CaCO_3 and

CaCl₂ are in the ashes. At 800°C the decarbonation of CaCO₃ is in progress, and its bands are disappearing, leaving only CaCl₂ bands. Chandler and others highlight the tendency of CaCl₂ to be hydrolyzed over its fusion point by water vapor when water-saturated air fluxes are used [7]. Nevertheless, with dry air fluxes at 950°C, CaCl₂ is a stable, transparent liquid, not showing any tendency to be hydrolyzed by the water vapor.

4.6.2 No reaction: Al(OH)₃

Al(OH)₃ starts the decompositions between 180°C and 200°C, releasing water [11]. Therefore, during the combustion, the actual substance in the matrix is alumina (Al₂O₃). Al₂O₃ is an inert substance not capable of reacting with HCl. Figure 2 shows the FTIR spectra of the ashes of formulation F50.1 at different temperatures. Figure 8 indicates that all spectra of Figure 2 have an excellent match with Al₂O₃ (see also Table 10), and therefore alumina is in the ashes obtained at 400°C, 500°C, 600°C, 800°C, and 950°C. The presence of Al is confirmed by XFR (Table 9), and Cl's presence is probably due to HCl trapped in the alumina surface. Additional measurements should clarify the presence of Cl in the F50.1 ashes. All these considerations explain why formulation 50.1 gives low and constant efficiency values at different temperatures (Table 13). Hence, Al(OH)₃ is an extremely weak acid scavenger at high temperatures due to the chemical inertia of its reaction product, Al₂O₃.

4.6.3 Single-step reaction: Mg(OH)₂

Mg(OH)₂ reacts fast with HCl generating MgCl₂. Mg(OH)₂ starts the decompositions between 300°C and 320°C, releasing water [11]. Thus, it is a perfect flame retardant; nevertheless, it is an ineffective acid scavenger at temperatures over 500°C. The formulation F50.2 gives maximum efficiency at 400°C, suddenly dropping down due to the instability of its reaction product, MgCl₂ (Table 13). Water vapor hydrolyzes MgCl₂ through the reactions reported in [8, 9]. The result is the production of 2 moles of HCl and 1 mole of MgO per mole of decomposing MgCl₂. The ashes analysis (FTIR measures in Figures 3, 9, 11, and Table 10) shows that the MgCl₂ hydrolysis is almost complete over 600 °C. Table 9 indicates that chlorine remains trapped in ashes (maybe passivation, preserving small quantities of MgCl₂ but further measurements should clarify this point).

All this puts in evidence a single-step reaction failing the scavenging at high temperature because Mg(OH)₂ yields an unstable product rereleasing HCl.

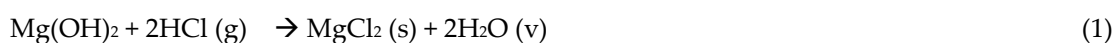
Table 8 shows how the formulations F50.2 and F50.3 reach almost the same pH and conductivities, indicating high acidity for different causes. As Al(OH)₃, Mg(OH)₂ is a very bad acid scavenger at high temperatures in the condensed phase, and therefore it does not show any effect in efficiency as temperature increases (Table 13). Again, a poor acid scavenger is usually terrible at all temperatures.

4.6.4 Single-step reaction: PCC

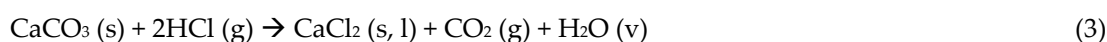
Tables 8 and 13 show that PCC alone is a good acid scavenger. PCC is not a strong base, and due to its small particle size, it can react with good efficiency, yielding CaCl₂, CO₂, and water. CaCl₂ is stable at 950°C. FTIR spectra confirm the formation of CaCl₂ and the disappearance of CaCO₃ bands (Figures 4, 7, 10, and Table 10) starting from 800 °C. The XRF measurements (Table 9) show the presence of chlorine and calcium. PCC shows good scavenging up to 800 °C.

4.6.5 Multiple-step reaction: PCC and Mg(OH)₂

Table 14 indicates that, if alone, Mg(OH)₂ shows a low impact on smoke acidity reduction. The efficiency of F50.2 is extremely low, 2.4 %. On the contrary, PCC performs well, and the efficiency reaches 18.4% in F50.3. Table 14 also shows that they have a strong synergism when used together. Figure 17 represents the efficiency at different ratios of loadings. Mg(OH)₂ and PCC reach maximum efficiency (28.8%) when PCC is 90 phr and Mg(OH)₂ 40 phr (F50.8). That efficiency is much more than the sum of the efficiency of Mg(OH)₂ and PCC alone (18.4 % and 2.4 %, respectively). The maximum is reached when the ratio PCC/ Mg(OH)₂ is 2.25, as Figure 17 shows. Probably the ratio that gives the maximum efficiency depends on the quantity of the pair and particle size of PCC and Mg(OH)₂ because both substantially affect efficiency. The synergism can be explained by a double-step reaction through which Mg(OH)₂ and PCC help each other. As a strong base, Mg(OH)₂ is the primary acid scavenger in the pyrolysis and combustion zone, and MgCl₂ is the main reaction product. The reactions during the matrix combustion are the following:



The second acid scavenger, PCC, reacts with HCl in less extent through reaction 3.



MgCl₂ is formed but decomposes between 350°C and 550 °C [8, 9] with a slow kinetic passing back its HCl to PCC. The synergism is explainable with a slow HCl release from MgCl₂ to PCC, enhancing the efficiency of PCC. All these aspects should be clarified deeper by FTIR-TGA measurements, pointing to the IR Cl and CO₂ signals in the range 350 °C – 550 °C. All these aspects will be discussed in a separate manuscript. Schemes 1-3 represent the hypothesis on the synergism between PCC and Mg(OH)₂.

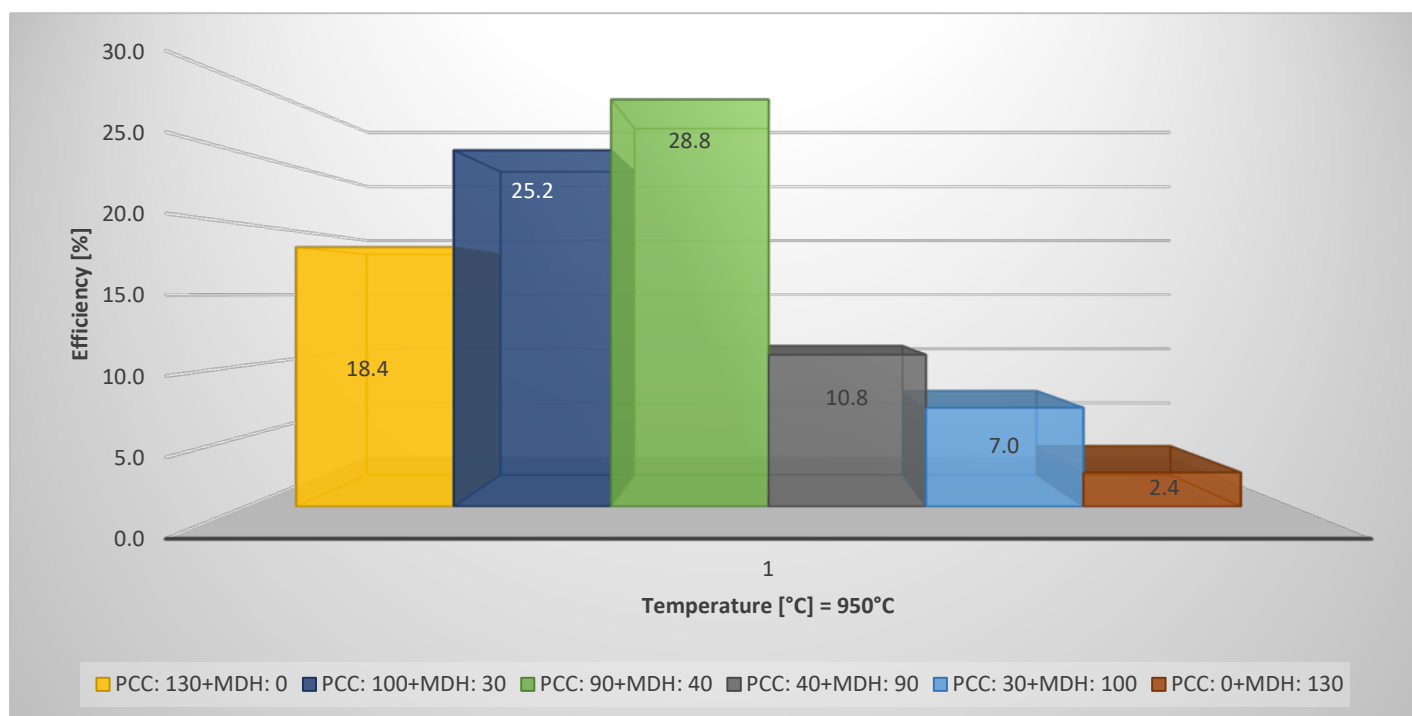
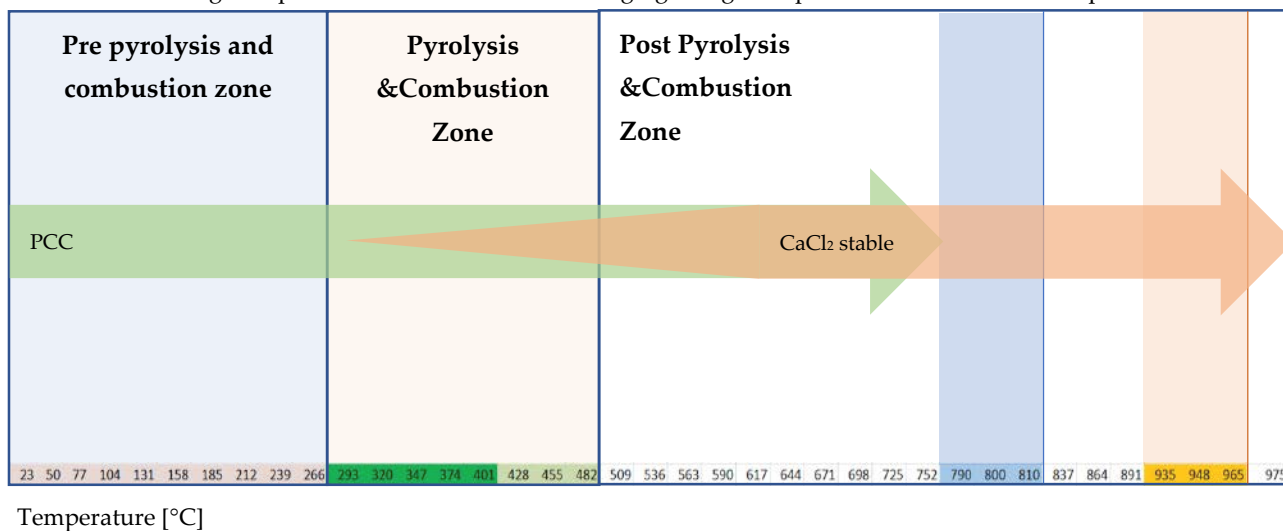
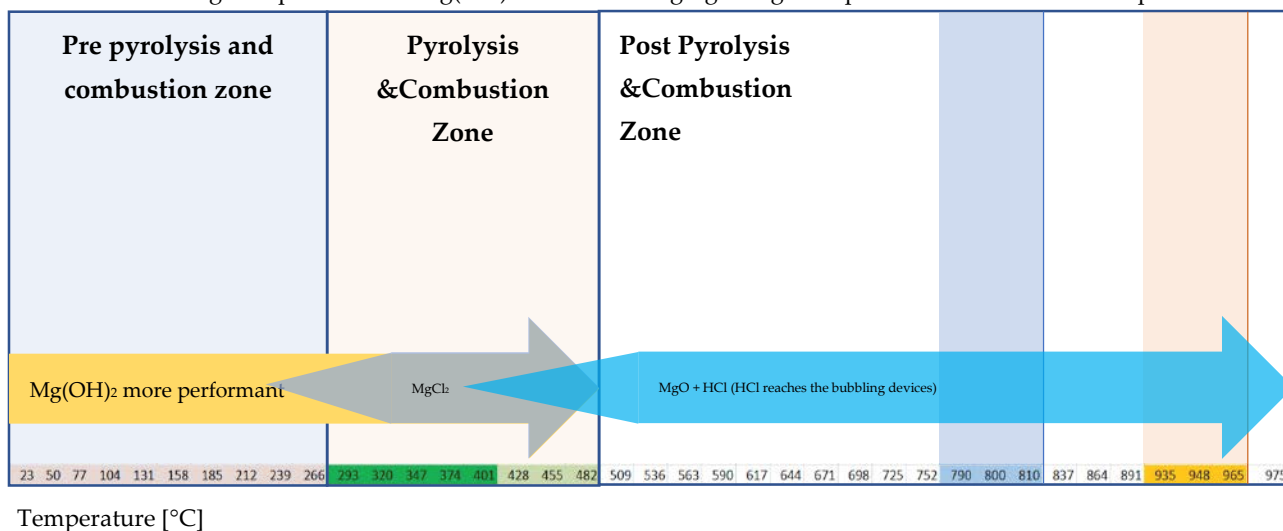
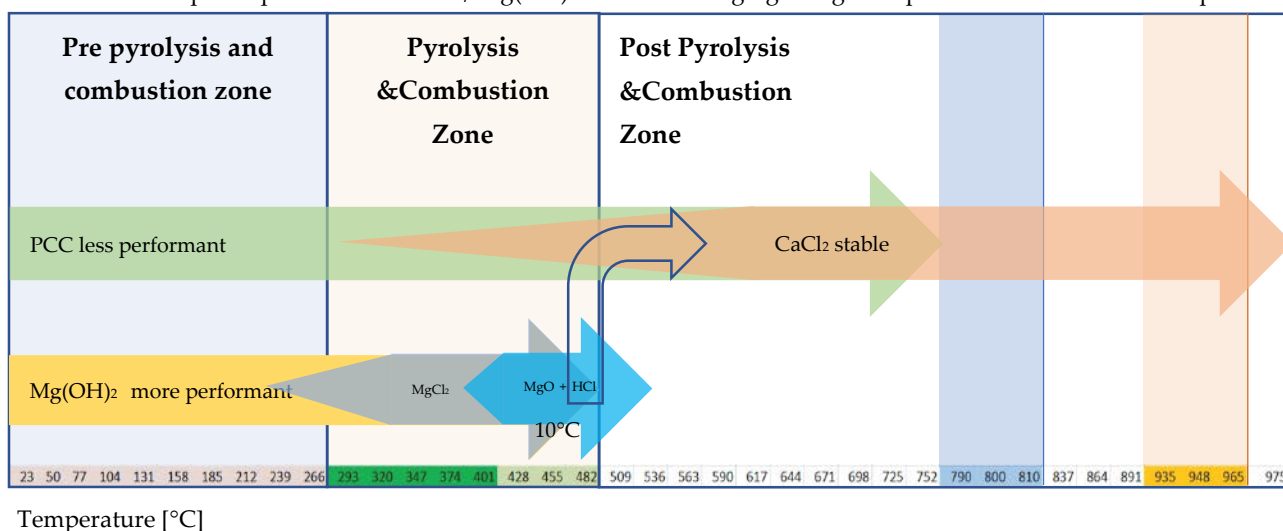


Figure 17. The efficiency for the formulations F50.6, F50.7, F50.8, F50.18, F50.19, F50.20. In the graph, MDH stands for Mg(OH)₂

Scheme 1. The single-step reaction of PCC in HCl scavenging at high temperatures in the condensed phase**Scheme 2.** The single-step reaction of Mg(OH)₂ in HCl scavenging at high temperatures in the condensed phase**Scheme 3.** Multiple-step reactions of PCC / Mg(OH)₂ in HCl scavenging at high temperatures in the condensed phase

5. Conclusions

Acid scavengers at high temperatures in the condensed phase differ in chemical nature and particle size, and some of them have been tested with different thermal profiles, performing EN 60754-2. $\text{Al}(\text{OH})_3$ and $\text{Mg}(\text{OH})_2$ are not efficient acid scavengers. When the matrix burns, the former generates an inert substance, alumina, while the latter reacts with HCl, yielding MgCl_2 , which decomposes over 500°C , rereleasing HCl.

GCC is not a good acid scavenger, but its efficiency increases as its particle size decreases. PCC is, therefore, more efficient in scavenging HCl than GCC. It reacts well with HCl in a single-step reaction, yielding CaCl_2 stable up to 950°C . When $\text{Mg}(\text{OH})_2$ and PCC work together, PCC scavenges the HCl from MgCl_2 decomposition. Probably the synergism happens because MgCl_2 releases HCl slower than the PVC matrix, and PCC can scavenge it more efficiently. Poor dispersion eliminates all synergism advantages when the quantity of $\text{Mg}(\text{OH})_2$ and PCC is too high.

Another aspect emerging from the data is the effect of temperature on the kinetic of HCl release. The higher the temperature, the lower the acid scavenger efficiency. This aspect confirms other researchers' past observations [7, 8]. The rapid HCl evolution causes the collapse of the efficiencies of acid scavengers at high temperatures. Acid scavengers are solid substances, and while some advantages are obtained when a lower particle size grade is used, they are annihilated when temperatures are too high.

In conclusion, it must be highlighted that different heating regimes give different acidity results. This aspect confirms how difficult it is to estimate the HCl concentration in real fire scenarios from bench-scale tests because HCl concentration in the gas phase will depend not only on its decay but also on temperatures reached in the fire.

Funding: This research received no external funding.

Acknowledgments: The author wants to acknowledge Ing. Ing. Carlo Ciotti, Ing. Marco Piana, all PVC Forum Italia and PVC4cables staff for their help and support, and Emma Sarti for the English text revision.

Conflicts of Interest: The authors declare that there is no conflict of interest regarding the publication of this paper.

References

1. Sarti, G., Piana, M. PVC in cables for building and construction. Can the "European approach" be considered a good example for other countries? *Academia Letters* **2022**, Article 5453, <https://doi.org/10.20935/AL5453>.
2. O'Mara, M. M., Pyrolysis–gas chromatographic analysis of poly(vinyl chloride). II. In situ absorption of HCl during pyrolysis and combustion of PVC. *Journal of Polymer Science Part A-1: Polymer Chemistry* **1971**, 9(5), 1387 – 1400, <https://doi.org/10.1002/pol.1971.150090519>.
3. S. K. Brown, K. G. Martin, Toxic gas and smoke measurement with the British Fire Propagation test. III: UPTV formulations with reduced HCl evolution. *Fire And Materials* **1985**, 9(2), 95-102, <https://doi.org/10.1002/fam.810090208>.
4. Commercial PCC purchased by Imerys. Available online: https://www.imerys-performance-minerals.com/system/files/2021-02/DATPCC_Winnofil_S_LSK_EN_2019-07.pdf (accessed on 12/08/2022)
5. G. Matthews, G. S. Plumper, Effects of calcium carbonate fillers on the behaviour of PVC in fires. *British Polymer Journal* **1981**, 13(1), 17-21, <https://doi.org/10.1002/pi.4980130105>.
6. G. Matthews, G. S. Plumper, Effects of fillers on and the role of hydrogen chloride in the behaviour of PVC in fires. *British Polymer Journal* **1984**, 16(1), 34-38, <https://doi.org/10.1002/pi.4980160107>.

-
7. Chandler L.A., Hirschler, Smith G. F., A heated tube furnace test for the emission of acid gas from PVC wire coating materials: effects of experimental procedures and mechanistic considerations. *European Polymer Journal* **1987**, 23 (1), 51-61, [https://doi.org/10.1016/0014-3057\(87\)90098-X](https://doi.org/10.1016/0014-3057(87)90098-X).
 8. Bassi, I., Characterization of PVC compounds and evaluation of their fire performance, focusing on the comparison between EN 60754-1 and EN 60754-2 in the assessment of the smoke acidity, Master degree Thesis, University of Bologna, Bologna, 10/2021. Available at: https://www.pvc4cables.org/images/assessment_of_the_smoke_acidity.pdf.
 9. Kipouros, G. J., Sadoway D. R., A thermochemical analysis of the production of anhydrous MgCl₂. *Journal of Light Metals* **2001**, 1, 111-117, [https://doi.org/10.1016/S1471-5317\(01\)00004-9](https://doi.org/10.1016/S1471-5317(01)00004-9).
 10. Galwey, A. K, Laverty, G. M., The thermal decomposition of magnesium chloride dihydrate. *Thermochimica Acta* 1989, 138(1), 115-127, [https://doi.org/10.1016/0040-6031\(89\)87246-6](https://doi.org/10.1016/0040-6031(89)87246-6).
 11. F. Laoutid, et al., New prospects in flame retardant polymer materials: from fundamentals to nanocomposites. *Material Science and Engineering Reports* 2009, 63(3), 100-125, <https://doi.org/10.1016/j.mser.2008.09.002>.